

## Surface roughness effect on KAGUYA LRS surface echo observation and its calibration

KOBAYASHI, Takao<sup>1\*</sup> ; LEE, Seung ryeol<sup>1</sup>

<sup>1</sup>Korea Institute of Geoscience and Mineral Resources

KAGUYA Lunar Radar Sounder (LRS) was an HF (5MHz) radar whose primary mission was to explore subsurface of the Moon. Its footprint covered whole surface of the Moon in its operation period. All the data was processed by applying Synthetic Aperture Radar (SAR) algorithm so that the signal-to-noise ratio of target echoes as well as the spatial resolution was improved.

The data was further processed to extract nadir surface echoes so that the surface property of the Moon was studied in a spectral range of the HF band. The physical property that can be known directly from the data was the apparent reflectivity of the lunar surface in the frequency range of the HF band: The data contains scattering effect of surface roughness due to the surface terrain. We need to separate this scattering effect from the data so that we can make quantitative evaluation of the surface reflectivity. In order to meet this requirement, we carried out simulation of KAGUYA LRS observation to evaluate the surface scattering effect due to the lunar surface terrain.

The simulation was based on Kirchhoff approximation method. The Lunar Imager/SpectroMeter (LISM) Digital Elevation Model (DEM) data was utilized to simulate actual lunar surface terrain. Flat surface observation was simulated as the reference case before the simulation of actual LRS observation was carried out. We assumed that the dielectric constant of the lunar surface material was 4.0.

Our simulation revealed that even a mare surface where the surface is often regarded to be flat certainly behaved as a rough surface which gave a rise to decrease of the nadir echo intensities for a few decibels in comparison to the flat surface reflection. This effect gives a significant influence on estimation of regolith thickness in maria. Newly estimated regolith thickness was approximately a meter smaller than previously estimated value: it turned out to be 6 - 7 m in Mare Imbrium.

Keywords: KAGUYA, LRS, HF radar, surface echo, scattering

## Determination of the dielectric constant of the lunar surface based on the radar echo intensity observed by the Kaguya

KUMAMOTO, Atsushi<sup>1\*</sup>; ISHIYAMA, Ken<sup>1</sup>; KOBAYASHI, Takao<sup>2</sup>; OSHIGAMI, Shoko<sup>3</sup>; HARUYAMA, Junichi<sup>4</sup>

<sup>1</sup>Tohoku Univ., <sup>2</sup>KIGAM, <sup>3</sup>NAOJ, <sup>4</sup>JAXA

In the planetary radar observation, echo power and delay time depend on the effective dielectric constant, or equivalent dielectric constant including the voids in the planetary uppermost media. As for the Moon, because there is almost no material whose dielectric constant is far from the basalt rocks, the effective dielectric constant of the lunar uppermost media is considered to depend mainly on their porosity. So if we can determine the effective dielectric constant of the lunar uppermost media, we can derive their bulk density, or density including the voids based on the empirical relation between the dielectric constant and bulk density of the Apollo samples [Carrier et al., 1991].

If we are going to use echo power for determination of the permittivity, we should note that the radar echo intensity depends not only on the dielectric constant but also on the roughness of the surface. Therefore, we have determined the permittivity of the lunar surface with considering the surface roughness. In the analysis, the dielectric constant is determined by using the radar echo intensity obtained by Kaguya Lunar Radar Sounder (LRS) [Ono et al, 2000; 2008; 2010], and the surface roughness parameters derived from Digital Terrain Model (DTM) based on Kaguya Terrain Camera (TC) observation [Haruyama et al., 2008]. The global distributions of the echo powers in a frequency range of 4-6 MHz were derived from the Kaguya/LRS dataset. We have used the intensity of off-nadir echoes in an incident angle from 5 to 15 degree. The reason why nadir echoes are not used in the analysis is because the echo intensity changes drastically in small incident angle range due to the poor range resolution from the spacecraft to the off-nadir reflection point. The echoes arrived after the arrival of the nadir surface echo were identified as off-nadir echoes in this study. In addition, we have also derived the global distribution of the surface roughness parameters. The RMS height of the surface can be obtained by  $\langle(z(x+L)-z(x))^2\rangle$ , where  $z(x)$  is height of the surface derived from the Kaguya TC/DTM,  $L$  is baseline length, and  $\langle\rangle$  denotes the average. If we assume the self-affine surface model, the roughness parameters  $H$  and  $s$  can be obtained by the least square fitting of the RMS heights to  $sL^H$ . The off-nadir surface echo power can be calculated based on the radar equation. Assuming Kirchhoff Approximation (KA), the backscattering coefficient in the radar equation can be obtained from the roughness parameters  $H$  and  $s$ , and assumed dielectric constant [cf. Bruzzone et al., 2011]. Using the backscattering coefficient, we can calculate the expected off-nadir surface echo powers. By performing the comparison between calculated and observed echo powers, we can determine most plausible dielectric constant. In the calculation of the echo powers, the transmitting loss of LRS have to be determined, which are however difficult to measure in the ground tests. So we estimated the transmitting loss to be 5.8 dB by assuming that the average dielectric constant is to be 5.3, which are derived from bulk density of 2.55 g/cm<sup>3</sup> in the highlands reported based on GRAIL observations[Wieczorek et al., 2013].

The obtained Hurst exponent  $H$  is less than 0.5 in the maria, and about 0.9 in the highland. The parameter  $s$  is about 1 in the maria, and about 0.3 in the highland. By applying the analysis method mentioned above, we could obtain the observed and calculated surface echo powers in the regions where  $H \sim 0.5$ , and  $H \sim 0.9$ . Based on them, we could estimate the average dielectric constant in the maria ( $H \sim 0.5$ ) to be 7, and that in the highland ( $H \sim 0.9$ ) to be 4. The bulk densities are therefore estimated to be 3.0g/cm<sup>3</sup> in the maria ( $H \sim 0.5$ ), and 2.1g/cm<sup>3</sup> in the highland. It suggests that there are more voids in the highland than in the maria due to longer exposure to the meteorite impacts.

Keywords: Kaguya (SELENE), Lunar Radar Sounder (LRS), Terrain Camera (TC), Surface roughness, Bulk density, Dielectric constant

## Tectonic evolution of Sinus Iridum and northwestern Imbrium regions

DAKE, Yuko<sup>1\*</sup>; YAMAJI, Atsushi<sup>1</sup>; SATO, Katsushi<sup>1</sup>; HARUYAMA, Junichi<sup>2</sup>; MOROTA, Tomokatsu<sup>3</sup>; OHTAKE, Makiko<sup>2</sup>; MATSUNAGA, Tsuneo<sup>4</sup>

<sup>1</sup>Graduate School of Science, Kyoto University, <sup>2</sup>Japan Aerospace Exploration Agency / Institute of Space and Astronautical Science, <sup>3</sup>Graduate School of Environmental Studies, Nagoya University, <sup>4</sup>National Institute for Environmental Studies

Tectonic features, including mare ridges and lobate scarps, visualize the permanent strains of the lunar crust, and show ancient stress field in the shallow part of the crust, which can further places constraint on global thermal history [1], orbital evolution [2] or basin-scale mascon loading [3, 4]. Their formation ages are clues to understand the origin of tectonic movements. The subsidence of mare basalts began to affect the lithosphere as soon as they were deposited, but global tectonics can affect it long after their deposition. Some of the lobate scarps were recently estimated to be younger than 0.1 Ga [5]. It was pointed out there are some mare ridges even on the youngest mare basalts. These young tectonic structures suggest their origins other than the mascon loading. However, the amount of contraction induced by mascon loading have not yet been elucidated. The formation age of each mare ridge is not well understood. In this study, we estimated the ages of mare ridges in northwestern Imbrium and Sinus Iridum regions.

By means of optical data taken by the cameras onboard SELENE, we estimated the depositional ages of mare units and constrained the formation ages of ridges. Mare basalt lavas were so inviscid that the lava field initially made level surfaces. Therefore, the ages of deformed and dammed mare units by tectonic structures help us to determine the upper and lower bound of formation ages of the structures. We defined geological units by spectral features. The absolute ages of the units were estimated by crater-size frequency distribution measurements, applicable to craters with diameters ranging from 0.25 to 1 km, where the production and chronology functions of Neukum and Ivanov [6, 7].

The prominent mare ridges in the study area are ENE-WSW trending ridge system, hereafter Ridge System A, and NE-SW trending ridge system, Ridge System B. They are located at just to the south of Promontorium Laplace. They are parts of the concentric ridge system of Mare Imbrium, suggesting that the ridges are results of mascon loading. The eastern part of Ridge System A branches into three relatively small ridges. There is a unit boundary runs along the southern foot of Ridge System A. Relatively Ti-poor basalt [8] makes up the ridge, and relatively Ti-rich one [8] lies on the plain at the foot of the ridge. This indicates that the unit was dammed by the ridge. Therefore, the upper and lower limits of ridge formation are determined by the ages of the deformed and dammed basalt units. As a result, we estimated the ages of nine units and constrained the ages of tectonic structures as follows. Western part of Ridge System A and northern part of Ridge System B were formed between 3.0 to 2.1 Ga and 3.3 to 2.1 Ga, respectively. However, Ridge System A partially reactivated and become higher after 2.1 Ga. The middle part of Ridge System B also partially reactivated after 2.1 Ga. The southern part of Ridge System B deforms the youngest basalt indicating it was formed after 2.1 Ga.

Most of mare ridges in the study area can not be explained by mascon loading, because the major subsidence by mare basalt was occurred before 3.0 Ga in Mare Imbrium. Accordingly, this area was tectonically active after the deposition of mare basalts.

We also report other young tectonic features, such as lobate scarps and arcuate rilles in the study area.

References: [1] Prichard M.E. and Stevenson D.J., in *Origin of the Earth and Moon*, Canup R.M. and Righter K., Eds. (Arizona Univ. Press, 2000), 179-196. [2] Melosh H. (1980) *Icarus*, 43, 334-337. [3] Solomon S.C. and Head J.W. (1979) *JGR*, 84,148-227. [4] Freed A.M. et al. (2001) *JGR*, 106, 20603-30620. [5] Watters T.R. et al. (2010) *Science*, 329, 936-940. [6] Neukum G. (1983) *Meteoritenbombardment und Datierung planetarer oberflächen*, Habil. Thesis, Univ. Munich. [7] Neukum G. et al. (2001) *Space Sci. Rev.* 96, 55-86. [8] Lucey P.G. et al. (1998) *JGR*, 103, E2, 3679.

Keywords: Mare ridges, Deformation ages, Crater ages, Mascon tectonics

## Evaluation of the horizontal shortening in the shallow part of the lunar crust

YAMAJI, Atsushi<sup>1\*</sup>; DAKE, Yuko<sup>1</sup>; SATO, Katsushi<sup>1</sup>; HARUYAMA, Junichi<sup>3</sup>; MOROTA, Tomokatsu<sup>2</sup>; OHTAKE, Makiko<sup>3</sup>; MATSUNAGA, Tsuneo<sup>4</sup>

<sup>1</sup>Division of Earth and Planetary Sciences, Kyoto University, <sup>2</sup>Graduate School of Environmental Studies, <sup>3</sup>Institute of Space and Astronautical Science, JAXA, <sup>4</sup>Center for Environmental Measurement and Analysis, National Institute for Environmental Studies

The topography of tectonic features in northwestern Imbrium and Sinus Iridum were studied in detail using SELENE-LISM data to estimate the horizontal shortening achieved by the formation of the features. As a result, it was found that the shortening by the formation of mare ridges was smaller than previous estimations by two orders of magnitudes except for a ridge, along which shortening was as large as ~500 m at maximum.

Keywords: tectonics, wrinkle ridge, graben, restoration

## Volcanic activity of lunar maria: Verification of super hot plume event at 2.0 Ga ago

KATO, Shinsuke<sup>1\*</sup> ; MOROTA, Tomokatsu<sup>1</sup> ; WATANABE, Sei-ichiro<sup>1</sup> ; YAMAGUCHI, Yasushi<sup>1</sup> ; OTAKE, Hisashi<sup>2</sup> ; OHTAKE, Makiko<sup>2</sup>

<sup>1</sup>Nagoya University Graduate School of Environmental Studies, <sup>2</sup>Japan Aerospace Exploration Agency

Because the Moon is an endmember of terrestrial planetary bodies, to understand the thermal evolution of the Moon is necessary for understanding that of terrestrial planetary bodies. However, the process of magma ocean solidification and the thermal and structural evolution of the lunar mantle are still unknown.

Lunar mare basalts provide insights into compositions and thermal history of lunar mantle. Using image data from orbital satellites, a considerable number of maria have been dated by various techniques such as crater degradation measurement, crater size?frequency measurement, and stratigraphic relationship. Mare basalt ages indicate that eruptive activity has a second peak at the end of lunar volcanism ( $\sim 2$  Ga), and the latest eruptions were limited in the Oceanus Procellarum and Mare Imbrium regions.

Using multiband images data obtained by SELENE/Kaguya, we have reinvestigated the relationship between titanium contents and eruption ages of mare basalts. Although the systematic relationship is not observed globally, an obvious increase in mean titanium content occurred at 2.3 Ga in the Oceanus Procellarum and Mare Imbrium regions, suggesting that the magma source changed at that time (hereafter, we call the volcanism before 2.3 Ga as Phase 1 volcanism, the volcanism after 2.3 Ga as Phase 2 volcanism.) The high-titanium basaltic eruption, which occurred at the late stage of mare volcanism, can be correlated with the second peak of volcanic activity at  $\sim 2$  Ga. The latest volcanic activity can be explained by the occurrence of a super hot plume originated from the core-mantle boundary.

To verify the super hot plume hypothesis, we calculate the difference between topography and selenoid in the mare region. We found a plateau structure around the center of the PKT region, whose the diameter is 1,000 km from southwest to northeast and 1,200 km from northwest to southeast and the altitude is 700 m. This plateau structure may be formed with ascending of super hot plume. Then, Phase 2 basaltic lava flows formed. If the ascending of super hot plume occurred  $\sim 2.0$  Ga ago, most mare formation had finished at that time and some transitional structures may have been left. In this presentation, we will discuss the relationship between Phase 2 high-titanium volcanisms and the super hot plume.

Keywords: Moon, lunar mare, titanium content, the Procellarum KREEP Terrane, super hot plume, selenoid

## Numerical models of mantle evolution in the moon

OGAWA, Masaki<sup>1\*</sup>

<sup>1</sup>Graduate School of Arts and Sciences, Univ. of Tokyo

Numerical models of magmatism in convecting mantle are presented to understand the lunar magmatism that was active for the first 1 Gyr but rapidly declined after that. In the model, the characteristic time of magmatism is on the order of several hundred million years, much longer than that of the model of magmatism on larger planets like Mars, because a positive feedback between magmatism and mantle convection does not work: Upwelling flow of mantle convection induces magma by decompression melting. The buoyancy of the magma enhances the upwelling flow itself, and hence makes magmatism vigorous in a large planet. This positive feedback, however, does not work in the moon because of its low Rayleigh number. The long characteristic time of magmatism in the model is consistent with observations. The suggested mild magmatism implies that the heat extraction by magmatism is inefficient in the moon. Since the convective heat extraction is also inefficient in the moon because of its low Rayleigh number, this inefficient heat extraction by magmatism suggests that the most important mechanism of mantle cooling in the moon is thermal diffusion. Indeed, the thickening of the lithosphere with time by thermal diffusion makes the activity of magmatism decline within the first 1 Gyr of its history regardless of the initial content of heat producing elements in the mantle and other parameters that controls magmatism and mantle convection in the models. It may be necessary to carry out further numerical studies that include the early chemical differentiation of the mantle by magma-ocean to understand the magmatism that remained active till 2 Ga locally in some areas of the moon.

Keywords: mantle evolution, mantle convection, magmatism, the moon

## Identification of secondary craters based on the Voronoi diagram of the lunar craters

KINOSHITA, Tatsuo<sup>1</sup> ; HONDA, Chikatoshi<sup>1\*</sup> ; HIRATA, Naru<sup>1</sup> ; MOROTA, Tomokatsu<sup>2</sup>

<sup>1</sup>The University of Aizu, <sup>2</sup>Graduate School of Environmental Studies, Nagoya University

We developed an automatic method for detecting crater clusters with crater spatial distribution based on the Area Voronoi tessellation technique. In the method based on the hierarchical cluster analysis, the evaluation of crater strongly depends on the closest one crater (or one cluster). In the method based on Voronoi tessellation on the other hand, it depends on the adjacent all craters. Since, this approach does not misjudge the pair craters evaluated cluster by the method based on the hierarchical cluster analysis. When a small crater is close adjacent a large crater, a boundary line of Voronoi tessellation is in the rim of the crater. This is different from the line a person pulls by intuition. So, we select Area Voronoi tessellation. For estimate an area of Voronoi, we adopted the wave front method (Watanabe and Murashima, 2006). We applied the Area Voronoi tessellation to observed crater spatial distribution. If the area of Voronoi cell is small, the crater becomes the candidate of the crater cluster. As a result, for the evaluation of crater spatial distribution, we propose that the Area Voronoi diagram is suitable to identify candidates of secondary crater.

Keywords: secondary crater, Voronoi diagram

## Development of a web application for dynamic analysis of the Kaguya Spectral Profiler data

SUGIMOTO, Kohei<sup>1</sup> ; HAYASHI, Yohei<sup>2</sup> ; OGAWA, Yoshiko<sup>1\*</sup> ; HIRATA, Naru<sup>1</sup> ; TERAZONO, Junya<sup>1</sup> ; DEMURA, Hirohide<sup>1</sup> ; MATSUNAGA, Tsuneo<sup>3</sup> ; YAMAMOTO, Satoru<sup>3</sup> ; YOKOTA, Yasuhiro<sup>3</sup> ; OHTAKE, Makiko<sup>4</sup> ; OTAKE, Hisashi<sup>4</sup>

<sup>1</sup>University of Aizu, <sup>2</sup>AIST, <sup>3</sup>NIES, <sup>4</sup>ISAS/JAXA

Kaguya is a Japanese lunar orbiter launched on September 14, 2007 and observed the moon for about 2 years. The Spectral Profiler (SP) on board Kaguya was a spectrometer which provided global data set of visible-near infrared continuous reflectance spectra of the Moon. GEKKO is a web-application used to visualize the data observed by SP. GEKKO displays the graph of SP spectra and tables of ancillary data with thumbnail images simultaneously taken by Kaguya imager/camera. The current version of GEKKO is very useful for viewing SP spectra, but does not include analysis functions.

The goal of this study is to develop a framework for implementing analysis functions of the SP data. For transferring the data from the client, the original GEKKO connects to the server using MapServer. However, in case of MapServer, the client-researchers can only analyze in a predetermined manner. Therefore, we prepared CGI scripts and incorporated them into GEKKO.

By using the new GEKKO system, the clients-researchers will be able to dynamically analyze the SP data. The clients can select, coordinate and add the functions according to their objectives. We prepared the basic functions commonly used for the spectral analysis, such as running average, normalization and also similarity measurement.

## Rock and mineral distribution of the lunar South Pole-Aitken basin

UEMOTO, Kisara<sup>1\*</sup> ; OHTAKE, Makiko<sup>2</sup> ; HARUYAMA, Junichi<sup>2</sup> ; YAMAMOTO, Satoru<sup>3</sup> ; NAKAMURA, Ryosuke<sup>4</sup> ; MATSUNAGA, Tsuneo<sup>3</sup> ; IWATA, Takahiro<sup>2</sup>

<sup>1</sup>The University of Tokyo, <sup>2</sup>Japan Aerospace Exploration Agency, <sup>3</sup>National Institute for Environmental Studies, <sup>4</sup>National Institute of Advanced Industrial Science and Technology

South Pole-Aitken (SPA) basin is one of the largest basin (2500 km in diameter [1] ) on the lunar farside. In pre-vious studies, it has been suggested that most of the crustal material was excavated and that the mantle materials have been exposed [e.g., 1]. Particularly, because this excavation was the biggest at the central area of the basin, mantle materials exposed. Mantle material of this area is melted by the basin impact and produced impact melt [e.g., 2], therefore we suggest that investigation within this impact melt area lead up to understand mantle material conpo-sition. However, because SPA is very old and large, we cannot identify the impact melt area. In our study, we pro-duce a new mineralogical map of SPA basin interior, based on data derived from SELENE Multiband Imager (MI). In particular, we investigated mineralogy within the central depression of SPA by iron and titanium concentration and altitude data derived from SELENE. Using these method, we identified the impact melt area of SPA.

We produced a mineralogical map within the central depression of SPA. As a result, we classified into three mineral type layers on this map ; low-Ca pyroxene layer, high-Ca pyroxene layer and very high-Ca pyroxene layer. From correlations of these layers and occurrences, we created the column diagrams of respective areas. Then, we suggested origins of these mineral type layers : The high-Ca pyroxene layer is impact melt area of the basin. The low-Ca pyroxene layer and the very high-Ca pyroxene layer is the ejecta of SPA basin and mare erupted after SPA basin formation, respectively. In fact, the area of the high-Ca pyroxene layer is impact melt area of SPA. In the fu-ture work, we will analyze mineral and chemical compositions within this area.

References: [1] Spudis et al., 1994. [2] Pieters et al., 2000

Keywords: South Pole-Aitken, lunar, rock, mineral

## Global Distribution Trend of High-Ca Pyroxene on the Lunar Highland by Satellite Hyperspectral Remote Sensing

YAMAMOTO, Satoru<sup>1\*</sup> ; NAKAMURA, Ryosuke<sup>2</sup> ; MATSUNAGA, Tsuneo<sup>1</sup> ; OGAWA, Yoshiko<sup>3</sup> ; ISHIHARA, Yoshiaki<sup>4</sup> ; MOROTA, Tomokatsu<sup>5</sup> ; HIRATA, Naru<sup>3</sup> ; OHTAKE, Makiko<sup>4</sup> ; HIROI, Takahiro<sup>6</sup> ; YOKOTA, Yasuhiro<sup>1</sup> ; HARUYAMA, Junichi<sup>4</sup>

<sup>1</sup>NIES, <sup>2</sup>AIST, <sup>3</sup>Univ. of Aizu, <sup>4</sup>JAXA, <sup>5</sup>Nagoya Univ., <sup>6</sup>Brown Univ.

The studies using the spectral data obtained by Spectral Profiler (SP) and Multiband Imager (MI) onboard the Japanese lunar explorer SELENE/Kaguya revealed the global distributions of the purest anorthosite (PAN), olivine-rich materials, orthopyroxene-rich, and spinel-rich materials over the entire Moon. However, the global distribution of high-Ca pyroxene (HCP)-rich sites has been unclear so far. In addition to mare region, which is dominated by HCP, it has been reported that several ray craters on highland regions show HCP-dominant spectra. Thus, the global distribution of HCP-rich sites, especially for the lunar highland regions, would provide important information for the structure and evolution of the lunar crust and mantle. Thus, using the global data set of the SP, we conducted the global survey to find HCP-rich sites on the Moon, especially for the lunar highland regions. Here, we report the global distribution trend of the HCP-rich sites based on this survey.

Keywords: Remote-sensing, Hyperspectral, Kaguya

## Solidification of the lunar magma ocean suggested by composition of the highland crust

OHTAKE, Makiko<sup>1\*</sup>; KOBAYASHI, Shingo<sup>2</sup>; TAKEDA, Hiroshi<sup>3</sup>; MOROTA, Tomokatsu<sup>4</sup>; ISHIHARA, Yoshiaki<sup>1</sup>; MATSUNAGA, Tsuneo<sup>5</sup>; YOKOTA, Yasuhiro<sup>5</sup>; HARUYAMA, Junichi<sup>1</sup>; YAMAMOTO, Satoru<sup>5</sup>; OGAWA, Yoshiko<sup>6</sup>; KAROUJI, Yuzuru<sup>1</sup>; SAIKI, Kazuto<sup>7</sup>

<sup>1</sup>Japan Aerospace Exploration Agency, <sup>2</sup>National Institute of Radiological Sciences, <sup>3</sup>Chiba Inst. of Technology, <sup>4</sup>Nagoya University, <sup>5</sup>National Institute for Environmental Studies, <sup>6</sup>The University of Aizu, <sup>7</sup>Osaka University

Introduction: Previously we reported that highland materials with higher Mg# (Mg/[Mg+Fe] in mole percent in mafic minerals) (up to 80) than those on the lunar nearside were found on the lunar farside [1]. The observed higher Mg# on the lunar farside indicates that the farside crust consists of rocks that crystallized from less-evolved magma than the nearside crust. One of the other key parameters for evaluating solidification of the lunar magma ocean is Th abundance. Th is an incompatible element and concentrates in the liquidus phase when magma cools, therefore highland material that solidified earlier must have lower Th abundance than the highland material that solidified later. Th abundance distribution and its dichotomic nature were found to be lower on the farside than on the nearside [2].

If the dichotomic distribution of lunar highland Mg# and the Th abundance were formed by lunar magma ocean solidification, as the solidification proceeds, Mg# will decrease while Th abundance will increase, giving the two parameters a negative correlation. This study investigated the correlation of the two observed parameters of the lunar highland to validate the magma ocean origin of Mg# and Th abundance distribution on the lunar surface. We also tried to estimate the chemical composition of the lunar magma ocean by combining two remote-sensing data sets.

Method: Using Kaguya gamma-ray data, we derived the relative Th abundance (count of the observed gamma-ray data) map of the Moon as gridded data. We then derived the Mg# map of the lunar highland so that it had the same grid as the Th abundance map. For comparison with the derived Mg# and Th abundance correlation trend, we calculated the Mg# of the lunar magma ocean starting with different bulk chemical compositions by using the MELTS program [3]. The calculated starting magmatic compositions were bulk silicate Earth and bulk lunar magma ocean.

Results: The derived Mg# and Th concentration ratio of the same location indicates a negative correlation of the two parameters. In addition to the negative correlation, another interesting feature is that there seems to be two separate trends with lower and higher Th concentration ratios. Comparison of the observed Mg# and Th concentration ratio trend with that of the model calculation suggests that the observed data of the lower Th concentration ratio group matches the bulk silicate Earth composition better than the lunar magma ocean.

Discussion: The negative correlation of observed Mg# and Th concentration ratio suggests that current values of these parameters on the lunar surface are likely due to cooling of the lunar magma ocean as each location crystallized at a different solidification stage though the origin of the two apparent sets of the observed trends is not clear. The fact that the observed data of the lower Th concentration ratio group matches the bulk silicate Earth model better may imply that the chemical composition of the lunar magma ocean needs to be re-evaluated and that the Mg# of the actual bulk lunar magma ocean may be higher than previously estimated although we need to further evaluate the effect of calculation conditions. The possibly higher Mg# of the bulk lunar magma ocean agrees with the reported higher Mg# (up to 80) in the farside highland than previously estimated based on the nearside sampled FAN compositions.

[1] Ohtake, M. et al. (2012) *Nature GeoSci.* 5, 384-388. [2] Kobayashi, S. et al. (2012) *Earth Planet. Sci. Lett.* 337, 107-116. [3] Ghiorso and Sack (1995) *Contrib. Mineral. Petrol.* 119, 197-212.

Keywords: Moon, Kaguya, SELENE, Crust, Magma Ocean

## Plagioclase with High Ca Contents from the Central Farside Highland.

TAKEDA, Hiroshi<sup>1\*</sup> ; NAGAOKA, Hiroshi<sup>2</sup> ; KAROUJI, Yuzuru<sup>3</sup> ; OHTAKE, Makiko<sup>4</sup> ; YAZAWA, Yuuki<sup>5</sup> ; YAMAGUCHI, Akira<sup>6</sup>

<sup>1</sup>Graduate School of Sciences, The University of Tokyo, <sup>2</sup>Waseda Univ., <sup>3</sup>JAXA/ISAS, <sup>4</sup>JAXA/ISAS, <sup>5</sup>Faculty of Engineering, Chiba Institute of Technology, <sup>6</sup>National Inst. of Polar Research

Some lunar meteorites contain clasts of nearly pure calcic plagioclase with high An values and low FeO (1). We proposed that these meteorites are derived from the lunar farside on the basis of estimated low concentrations of Th and FeO by the remote sensing data on the farside of the Moon (2). The Lunar Magma Ocean (LMO) model deduced from the Apollo samples is not able to explain such dichotomy of the Moon. Nyquist et al. (3) performed Sm-Nd and Ar-Ar studies of pristine ferroan anorthosites (FANs) of the returned Apollo samples and showed that a whole rock Sm-Nd isochron for selected FANs yields an isochron age of 4.47 Ga. Mineralogical studies of lunar meteorites of the Dhofar 489 group (2) and Yamato 86032, all possibly from the farside highlands, showed some aspects of the farside crust. Nagaoka et al. (1) reported that many fragments in such meteorites contain clasts of nearly pure calcic plagioclase with high An values.

Mineralogy of magnesian anorthosite clasts in Dhofar 489, 309 and 307 (2) was used to deduce the ejection site of the Dhofar 489 group. Presence of fine-grained magnesian granulitic clast, and many crystalline clasts with rapid growth features were interpreted in terms of a large impact basin associated with small cratering. Among a few large basins of the farside, the Dirichlet-Jackson (DJ) basin has a few large craters on the floor, and the formation age by Morota et al. (4) is 4.25 Ga, which agrees with the Ar-Ar age (4.23 Ga) of Dhofar 489 (2). Based on the Th map made by KGRS, Kobayashi et al. (5) showed that the lowest Th regions in the lunar farside occurs near the equatorial region and noted that the regions well correspond to the high Mg number region (DJ) measured by SP, of the farside crust (6). These rocks with low Th may be crystallized from less-evolved magma than the nearside crust. Anorthosites composed of nearly pure anorthite (PAN) with low Th at many locations in the farside highlands and a map of the Mg numbers (6) also showed that the region around the DJ basin is consistent with the Mg numbers (70 to 76) of the magnesian anorthositic clast in Dhofar 489 (2). A large impact, which excavated a basin of the farside might have produced granulites in deep ejecta of a smaller impact.

We investigated a process of decomposition of Ca-rich plagioclase with fulvic acid, which is a complex natural organic acid produced in humified soils (7). The Ca ion released from plagioclase can be used to fix carbon dioxide as calcite as in oolites, and is useful for reducing carbon dioxide from the atmosphere on the Earth.

References: (1) Nagaoka H., Takeda H. et al. (2012) 75th Ann. Meet. Meteorit Soc. Abstr no. 5197. (2) Takeda et al. (2006) Earth Planet Sci Lett 247, 171-184. (3) Nyquist L. E. et al (2013) LPSC 45th no. 1125. (4) Morota T. et al. (2011) JGU Meeting, PPS024-10. (5) Kobayashi S. et al. (2012) EPSL, 337-338, 10-16. (6) Ohtake M. et al. (2012) Nature Geosci., 5, 384-388. (7) Yazawa Y. et al. (2012) Chapter. 5, in Moon, B. Viorel Ed., XXXVIII, 750 p, 105-138, Springer.

Keywords: plagioclase, lunar crust, farside highland, resource utilization

## Volatile accretion on the Moon - A clue for the emergence of a habitable Earth.

HASHIZUME, Ko<sup>1\*</sup> ; HARUYAMA, Junichi<sup>2</sup>

<sup>1</sup>Osaka University, Graduate School of Science, <sup>2</sup>Japan Aerospace Exploration Agency / Institute of Space and Astronautical Science

I would like to introduce the recent advancement in deciphering the information on accretion of planetary volatile compounds to the moon using lunar regolith samples. I will also make a brief comment on the future lunar explorations, toward a better understanding of volatile accretion to the early Earth-Moon system that possibly lead to the emergence of the habitable Earth.

Keywords: Lunar Regolith, Volatile Compound, Isotope Composition, Accretion Rate

## Extraterrestrial solidified materials with multi-mixture on the Moon

MIURA, Yasunori<sup>1\*</sup>

<sup>1</sup>In & Out Universities

The results of the present study are summarized as follows:

1) Study of the Moon provides largely valuable information on formation processes of primordial Earth and extraterrestrial celestial-bodies.

2) Identification of crystalline solids are almost similar between the Moon and Earth, though the Moon rocks might be formed by similar formation processes of terrestrial (Earth) rocks based on the crystalline parts. However, extraterrestrial solids are mixtures of multiple states shown as amorphous solids.

3) Formation of quasi-spherical Moon body formed mainly by impact-related melting process is found as heterogeneous and irregular distribution of lunar rocks with impact craters.

4) Fluid-bearing depositions irregularly distributed on the surface and interior of the Moon are largely based on storages on the interior formed by solidified mixtures of multiple states triggered by impact process on the Moon.

5) Different processes of solids between the Moon and Earth can be observed silica Si-O frameworks which can be obtained by the ion bombardment experiments. Crystalline rocks with hard silicate structures show higher ion-peaks of alkali ions (Na, K and Ca etc.), whereas solid-aggregates of the Moon rocks show higher ion-peaks of Si and Al ions which are easily destroyed by ion bombardment relatively.

6) Ion-peaks by the sputtering of Earth impact-breccias are clearly higher than those of the Moon breccias, which main differences are not rock textures but atomic bonding.

7) The air- and water-less Moon with solidified materials with multi-states is formed from nano-grains to macroscopic rocks by impact-related evolution process.

8) The primordial planet Earth with remained heterogeneous surface by impact-related process is considered to be different cyclic system of three states (air, liquid and solid) with macro-life activity which is formed by huge production from the interior triggered by huge collision process of the giant impact.

Keywords: the Moon, mixture, solidified material, material state, silicate framework, ion bombardment run

## Re-examination of Excavation Cavity of the Impact Basins of the Moon based on GRAIL based Crustal Thickness Model

ISHIHARA, Yoshiaki<sup>1\*</sup> ; NAKAMURA, Ryosuke<sup>2</sup>

<sup>1</sup>JAXA, <sup>2</sup>AIST

Large impact features, whose diameters are more than hundreds of kilometers, are called impact basins. Large impact basins can provide comparatively clear information of the cratering process and/or constrain the lunar thermal history. The internal or subsurface structures of basins can be assessed through an analysis of their associated gravitational and topographic signatures. The recently Kaguya/SELENE mission has improved the crustal thickness model not only for the nearside but also for the farside based on the first direct farside gravity and global topography mapping. Moreover most recent GRAIL mission vastly improved spatial resolution and overall accuracy of the lunar gravity models and lunar crustal thickness models. The GRAIL crustal thickness model gives us the opportunity to re-analyse excavation depth and diameter of basin forming impact processes anywhere on the Moon with improved accuracy. This study uses the GRAIL crustal thickness model, to reconstruct the excavation cavity geometry of large impact basins on the Moon.

Our method of reconstructing the excavation cavity of large impact basins is fairly simple. We assume that the thinned crust and uplifted Moho beneath features is a direct consequence of (1) the amount of crustal material excavated during the cratering process and (2) the subsequent rebound of the crater (basin) floor. We first construct azimuthally averaged profiles for the surface topography, mare thickness and subsurface structure of the Moho for each basin. Next, we restored the uplifted Moho and overlying crust to its pre-impact position. Estimating procedures of pre-impact position is almost the same as previous analysis. After removing mare fill, this process resulted in a roughly parabolic surface depression, that we interpret as being the first-order representation of the basin's excavation cavity.

One of the most important values of understanding the large impact basin is the depth-to-diameter ratio of the excavation cavity. We examine the depth versus the diameter of our reconstructed excavation cavities (excluding the Imbrium Basin and the South Pole-Aitken Basin). It seems that up to 400 km cavity diameter, the depth (hex) and diameter (Dex) are linearly related. Further more, the linear relationship ( $hex/Dex=0.079\pm 0.006$ ) is almost consistent with, though slightly smaller than, the value for craters orders of magnitude smaller in size ( $hex/Dex=0.1$ ), suggesting that proportional scaling is valid for basin scale impact structures except the largest impact structures on the Moon. One of the reasons of smaller depth-to-diameter ratio are probably effects due to the post impact modifications. Impact basins which has excavation cavity diameter larger than 400 km show the different state. The average crustal thickness of GRAIL lunar crustal thickness model is 34 to 43 km. So excavation cavity diameter of 400 km is located the regime boundary between the excavation/melting cavity within crust regime and the excavation/melting cavity exceed the Moho interface regime.

Keywords: Impact Basin, Excavation Cavity, Melting Cavity, Moon

## Lunar gravity anomaly recovery with the GRAIL level-1b and level-2 data

HASHIMOTO, Mina<sup>1\*</sup> ; HEKI, Kosuke<sup>1</sup>

<sup>1</sup>Department of Natural History Sciences, Faculty of Science, Hokkaido University

First, we will talk about the lunar gravity anomaly recovery with the GRAIL level-1b data. Among several global lunar gravity field models available now, GRAIL offers the highest resolution. The Doppler tracking between Earth-based stations and lunar satellites can directly observe gravity field of the lunar nearside. SELENE could measure the farside, for the first time, by inter-satellite tracking using the high-altitude relay satellite. GRAIL employs the low-low inter-satellite tracking method, often called as " Tom and Jerry ". This is similar to GRACE, the twin satellites for the gravimetry of the earth. It observes the gravity field by ranging between the satellites using microwave. In this way, GRAIL got the global lunar gravity anomaly map. In our study, we use the GRAIL level-1b and level-2 data. Both data have become open to public at the PDS Geoscience Node at the Washington University, Saint Lewis. The level-1b data include satellite position data compiled as the GNV1b files, and inter-satellite ranging data (ranges, range rates, and range accelerations every five seconds) are compiled in the KBR1b files. In this study, we used these two data sets and estimated the mass distribution on the moon. We remodeled the moon's gravity anomaly program of the Lunar Prospector developed by Sugano and Heki (EPS 2004; GRL 2005). Using this program, we estimated the gravity anomaly of the specific parts of the lunar surface. We found the Level-1b data are able to recover them clearly. Then, we will introduce the next-stage study by using the GRAIL level-2 data set, and explain the scientific targets of our study. Recent study (Miljkovi?, K. et al., 2013) suggested that the size and depth of the crater depends on the mantle temperature as well as the size and speed of the projectile. We here study the gravity signatures of small to medium sized craters, and will find systematic difference between the lunar near and far sides.

## Consideration of the seismic moment distribution of deep moonquake and the lunar deep structure

YAMADA, Ryuhei<sup>1\*</sup> ; NODA, Hiroto<sup>1</sup> ; ARAKI, Hiroshi<sup>1</sup>

<sup>1</sup>National Astronomical Observatory of Japan / RISE Project

The Apollo seismic network consists of 4 seismic stations (Apollo12, 14, 15 and 16) have observed deep moonquakes which occur repeatedly from specific source regions at depth of 700-1200 km in the lunar deep region. The deep moonquake occurs periodically related with positions of the Earth, the Moon and the Sun; that is tidal forces (e.g., Lammlein, 1977, Bulow et al., 2007). The 106 deep moonquake sources are currently located (Nakamura, 2005), the activity and largeness of the deep event and maybe occurrence mechanism are different among the sources (Araki, 2001).

Yamada et al., (2013) have investigated seismic moment of each deep event occurred from active and well-located 15 deep sources from analysis of data obtained in Apollo 12 station. To derive the seismic moment, we have to correct for characteristics of the Apollo seismometers, elastic and attenuation parameters of the lunar interior where the seismic phase passes, geometrical spreading and radiation pattern of the fault at source region from amplitude of the seismic event (Goins et al., 1981). In Yamada et al., (2013), recent lunar interior model VPREMOON (Garcia et al., 2013) are used, and the results have shown that the values of seismic moments are different among active 15 sources and far deep sources occur the events which have larger seismic moment than near sources.

In this study, we have derived the seismic moments of identical deep events observed in Apollo 15 and 16 stations to verify the previous results derived from analysis of Apollo 12 data. This analysis indicates that the values of seismic moments derived from each station data are respectively different from even if the events are identical. We found a tendency which deep moonquakes occur from far sources indicates larger differences in seismic moments derived from each station data than near source events. This may mean that the recent lunar interior model applied in this study has some problems. Especially, seismic quality factor in the mantle mainly affects on amplitudes of the seismic events. Previous studies (e.g., Nakamura and Koyama, 1982) have described that values of seismic quality factor had large uncertainty in lunar deep region. We, therefore, derived appropriate seismic quality factor so as to minimize differences of the seismic moments derived from each station data. In this analysis, we considered effects of possible radiation patterns because these values also have large uncertainty and effect on derivation of the seismic moments. We will report and discuss our new seismic moment distribution of deep moonquakes and new values of seismic quality factor in this presentation.

**Keywords:** Deep Moonquake, Seismic Moment, Lunar Seismic Activity, Lunar Mantle, Lunar Seismic Quality Factor, Lunar Deep Structure

## Variation of the ionized lunar sodium and potassium exosphere

YOKOTA, Shoichiro<sup>1\*</sup> ; SAITO, Yoshifumi<sup>1</sup> ; ASAMURA, Kazushi<sup>1</sup> ; NISHINO, Masaki<sup>n2</sup> ; TSUNAKAWA, Hideo<sup>3</sup>

<sup>1</sup>ISAS/JAXA, <sup>2</sup>STE Lab., <sup>3</sup>Tokyo Institute of Tech.

Lunar exosphere has been observed and studied on many occasions by ground-based telescopes since the discovery of surface-bounded alkali exosphere. The observed exospheric components were alkali atoms such as Na and K because the emission lines are much brighter than for other conceivable components. The structure, source, and the transport mechanisms of the lunar exosphere have been discussed based on these ground-based observations of the alkali atoms. As for the source mechanism of the thin lunar alkali exosphere, five processes were proposed as follows: thermal desorption, electron-stimulated desorption (ESD), photon-stimulated desorption (PSD), ion-induced desorption (sputtering), and vaporization by micrometeoroid impacts. Structure of the lunar exosphere gives us the key parameters to investigate the source mechanism. The observed Na exosphere distribution suggested that PSD and/or sputtering do not simply release the exospheric particles. Since PSD is capable of releasing alkali atoms only out of very shallow region in the lunar soils, PSD has relatively limited store of the exospheric particles in the lunar surface. If there was no replenishing process, PSD would deplete surface alkalis. We present latitude and longitude distributions of Na<sup>+</sup> and K<sup>+</sup> fluxes from the Moon derived from the Kaguya low-energy ion data. Although the latitude distribution agrees with the previous ground-based telescope observations, dawn-dusk asymmetry has been found in the longitude distribution. Our model of the lunar surface abundance and yield of Na and K demonstrates that the abundance decreases to around 50%, at dusk compared to that at dawn due to the emission of the exospheric particles. It is also implicated that the surface abundance of Na and K need to be supplied during the night in order to explain the observed lunar exosphere with the dawn-dusk asymmetry.

Keywords: Moon, Exosphere, Alkali atmosphere, Mass analyses

## Various appearances of whistler-mode waves observed near the Moon in the solar wind

TSUGAWA, Yasunori<sup>1\*</sup>; KATOH, Yuto<sup>1</sup>; TERADA, Naoki<sup>1</sup>; TSUNAKAWA, Hideo<sup>2</sup>; TAKAHASHI, Futoshi<sup>2</sup>; SHIBUYA, Hidetoshi<sup>3</sup>; SHIMIZU, Hisayoshi<sup>4</sup>; MATSUSHIMA, Masaki<sup>2</sup>

<sup>1</sup>Department of Geophysics, Tohoku University, <sup>2</sup>Department of Earth and Planetary Sciences, Tokyo Institute of Technology, <sup>3</sup>Department of Earth and Environmental Sciences, Kumamoto University, <sup>4</sup>Earthquake Research Institute, University of Tokyo

Narrowband whistler-mode waves whose frequencies close to 1 Hz have been observed near the Moon [Farrell et al., 1996; Nakagawa et al., 2003; Halekas et al., 2006; Tsugawa et al., 2011]. Broadband whistler-mode waves in the frequencies up to about 10 Hz with no preferred polarity have also been observed near the Moon [Halekas et al., 2008; Nakagawa et al., 2011, Tsugawa et al., 2012]. In addition, the lunar magnetometer (LMAG) aboard Kaguya detected right-hand polarized broadband waves, which is relatively weak and appears in the frequency range of several Hz. Since the angle between the wave vector and the sunward direction is large, the waves are not significantly Doppler shifted, indicating that they are whistler-mode waves. We also reveal the existence of harmonic waves whose fundamental waves appear in the frequencies near 1-2 Hz. The fundamental waves resemble the narrowband whistler-mode waves.

We construct criteria to select these waves and perform statistical analyses. Based on the statistical properties, we suggest possible scenarios of the generation and propagation of the four types of waves around the Moon. Whistler-mode waves in the frequency near the lower hybrid frequency generated through the reflection of ions by the Moon would be observed as (1) the narrowband waves in the spacecraft frame when the group velocity vector points to the sunward and is cancelled by the solar wind velocity, as (2) the broadband waves in the interaction region with various wave components, as (3) the right-hand polarized broadband waves when the wave vector points perpendicular to the sunward, and as (4) the harmonic waves in the same condition with NR with a large compressional component enough to be steepened.

## Detection experiment of Ar emission lines for K-Ar dating using Laser-Induced Break-down Spectroscopy

OKUMURA, Yu<sup>1\*</sup> ; SHIBASAKI, Kazuo<sup>1</sup> ; OISHI, Takahiro<sup>1</sup> ; CHO, Yuichiro<sup>2</sup> ; KAMEDA, Shingo<sup>1</sup> ; MIBE, Kenji<sup>2</sup> ; MIURA, Yayoi N.<sup>2</sup> ; SUGITA, Seiji<sup>2</sup>

<sup>1</sup>Rikkyo University, <sup>2</sup>The University of Tokyo

JAXA is currently planning the lunar lander SELENE-2 project, a follow-up mission of SELENE. This project involves the dispatch of a lunar rover to investigate the lunar surface and rocks. We propose Laser-Induced Breakdown Spectroscopy (LIBS) as an instrument for mounting rovers. The LIBS conducts in-situ analysis of elemental composition.

The LIBS instrument uses a high intensity laser pulse and induced plasma. The plasma emits energy in the form of photons. The spectroscopic analysis of the plasma enables the determination of the elemental composition.

K-Ar dating is a radiometric method used in geochronology. It is based on the measurement of the product of the radioactive decay of <sup>40</sup>K into <sup>40</sup>Ar with a half-life of 1.25 Gyr. K is found in many rocks. Therefore, we can determine the solidification age of rocks by measuring the ratio of <sup>40</sup>K to <sup>40</sup>Ar in the rock. In the existing K-Ar dating method, K is measured using LIBS and Ar is measured using quadrupole mass spectrometry (QMS); thus, the method needs two measuring instruments. Our method can be applied to measure both K and Ar using only LIBS. Therefore, the instrument weight will be reduced if our method is applied successfully. The Curiosity rover, a part of NASA's Mars Science Laboratory mission, used LIBS to obtain the spectra of rocks present on the surface of Mars. The Curiosity rover's LIBS instrument detected K in the rocks. However, Ar has not been detected using LIBS. We conducted experiments to detect the Ar emission lines using LIBS.

Commonly, the temperature of plasma induced using LIBS is approximately 1eV (11600K) in the atmosphere. When temperature of plasma was 1eV, we expected that it is possible to detect the Ar emission lines at the wavelengths of 104.8nm and 106.7nm in the vacuum ultraviolet spectral range because no emission lines of neutrals and singly-charged ions of major elements exist in the range. However, as a result, we found that the plasma temperature might be several tens of eV in vacuum. We found that relative intensity of multiply-charged ions (e.g. Si(IV), Fe(II)) emission lines is much stronger than the Ar emission lines. Therefore, we decreased the temperature of plasma in vacuum by decreasing the pulse laser intensity and conducted experiments. In addition, we conducted experiments to investigate the Ar emission lines, which we might be able to detect when the plasma temperature is higher than 1eV, in the vacuum ultraviolet (VUV)-near infrared (NIR) range in vacuum.

Keywords: LIBS, elemental compositions, K-Ar dating, Planetary Explora, Moon

## Unprecedented Zipangu Underworld of the Moon Exploration (UZUME)

HARUYAMA, Junichi<sup>1\*</sup>; KAWANO, Isao<sup>1</sup>; KUBOTA, Takashi<sup>1</sup>; OTSUKI, Masatsugu<sup>1</sup>; NISHIBORI, Toshiyuki<sup>1</sup>; IWATA, Takahiro<sup>1</sup>; ISHIHARA, Yoshiaki<sup>1</sup>; YAMAMOTO, Yukio<sup>1</sup>; NAGAMATSU, Aiko<sup>1</sup>; HASENAKA, Toshiaki<sup>3</sup>; SHIMIZU, Hisayoshi<sup>4</sup>; MOROTA, Tomokatsu<sup>5</sup>; MICHIKAMI, Tatsuhiro<sup>6</sup>; SHIRAO, Motomaro<sup>7</sup>; MIYAMOTO, Hideaki<sup>4</sup>; KOBAYASHI, Kensei<sup>2</sup>; YAMAMOTO, Satoru<sup>8</sup>; YOKOTA, Yasuhiro<sup>8</sup>; HASHIZUME, Ko<sup>9</sup>; SAIKI, Kazuto<sup>9</sup>; KOMATSU, Goro<sup>10</sup>

<sup>1</sup>Japan Aerospace Exploration Agency, <sup>2</sup>Yokohama National University, <sup>3</sup>Kumamoto University, <sup>4</sup>University of Tokyo, <sup>5</sup>Nagoya University, <sup>6</sup>Kinki University, <sup>7</sup>Planetary Geology Institute, <sup>8</sup>National Institute for Environmental Studies, <sup>9</sup>Osaka University, <sup>10</sup>Universita d'Annunzio

Japanese lunar explorer SELENE (Kaguya) discovered gigantic vertical holes of 100 m in diameters and depths in the Marius Hills, Mare Tranquillitatis, and Mare Ingenii of the Moon. These holes are possibly skylights of underground large caverns such as lava tubes, magma chambers, or faults. There are lots of scientific interests on the holes and associating caverns. In addition, these holes and underground structures are the best candidate locations for future lunar base. Similar holes have been also found on the Mars. The caverns connecting to the Martian holes may be the best place for Martian lives to emerge, evolve and survive because of their safer conditions than the Martian surface. We are now planning to establish a project working group to explore the lunar holes and caverns associating to the holes. We call the project as UZUME (Unprecedented Zipangu Underworld of the Moon Exploration).

Keywords: Moon, SELENE, hole, cavern

## Development of ILOM using DOE and situation of trial manufacturing of DOE

KASHIMA, Shingo<sup>1\*</sup> ; ARAKI, Hiroshi<sup>1</sup> ; HANADA, Hideo<sup>1</sup> ; TSURUTA, Seiitsu<sup>1</sup> ; SUZUKI, Hirofumi<sup>2</sup> ; YASUDA, Susumu<sup>3</sup> ; UTSUNOMIYA, Shin<sup>3</sup>

<sup>1</sup>RISE Project Office, National Astronomical Observatory of Japan, <sup>2</sup>Mechanical Engg., Chubu University, <sup>3</sup>Japan Aerospace Exploration Agency

We have a plan to install the photo-zenith telescope on the moon as part of a next SELENE project. The purpose is to explain the internal structure and the origin of the moon by measuring the small vibration and movement with very high accuracy. In this presentation, we show the development of ILOM using DOE that actualize the very high performance, i.e., 1 mas, in the severe thermal condition of the moon and show the situation of the trial manufacturing of DOE that is the key technology of this telescope.

Keywords: ILOM, DOE, SELENE

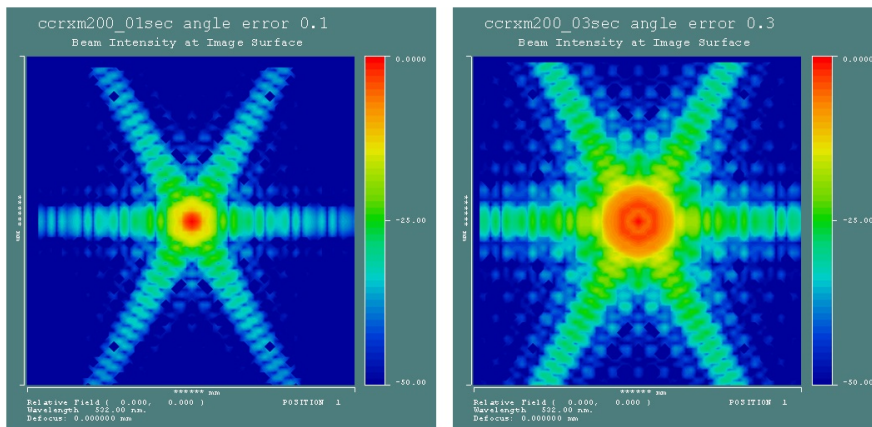
## Angle, deformation and DAO (Dihedral Angle Off-set) Analysys of the corner cube mirror for LL

KASHIMA, Shingo<sup>1\*</sup> ; NODA, Hiroto<sup>1</sup> ; ARAKI, Hiroshi<sup>1</sup> ; HANADA, Hideo<sup>1</sup> ; KUNIMORI, Hiroo<sup>2</sup> ; OTSUBO, Toshimichi<sup>3</sup>

<sup>1</sup>RISE Project Office, National Astronomical Observatory of Japan, <sup>2</sup>National Institute of Information and Communications Technology, <sup>3</sup>Social Sciences, Hitotsubashi University

We have a plan to install the corner cube mirror which has about 20cm aperture on the moon as part of a next SELENE project. The purpose is to explain the internal structure and the origin of the moon by measuring and analysing the distance between the moon and the earth with cm order accuracy. In order to actualize such a precise measurement, we have to manufacture the CCM with 0.1 sec angular precision and less the  $\lambda/10$  flatness for the mirror surface. In this presentation, we show the optical response analysis for deriving these degree of precision.

Keywords: LLR, CCM, SELENE



## Development of the Retroreflector on the Moon for the Future Lunar Laser Ranging

ARAKI, Hiroshi<sup>1\*</sup>; KASHIMA, Shingo<sup>1</sup>; NODA, Hirotomo<sup>1</sup>; KUNIMORI, Hiroo<sup>2</sup>; CHIBA, Kouta<sup>3</sup>; OTSUBO, Toshimichi<sup>4</sup>; UTSUNOMIYA, Makoto<sup>5</sup>; MATSUMOTO, Yoshiaki<sup>6</sup>

<sup>1</sup>National Astronomical Observatory of Japan, <sup>2</sup>National Institute of Communication and Technology, <sup>3</sup>Iwate University, <sup>4</sup>Hitotsubashi University, <sup>5</sup>Japan Aerospace Exploration Agency, <sup>6</sup>PLANET Co. Ltd.

Lunar Laser Ranging (LLR) data are important for the investigations of the lunar rotation, tide, and lunar deep interior structure. The range accuracy of LLR has been less than 2 cm for the last 20 years due to the progress of laser transmit/receive system on the ground stations and the atmospheric signal delay model, however, one order or more accurate ranging than 2cm is needed for better understanding of the lunar deep interior. We are developing 'single aperture and hollow' retroreflector (Corner Cube Mirror; CCM) to be aboard future lunar landing missions. The aperture of CCM is 20cm because the reflection efficiency of that size is found to be higher than that of Apollo 11 array CCP (Corner Cube Prism). For the CCM ultra low expansion glass-ceramic (ClearCeramRZ-EX, OHARA Inc.; hereafter CCZ-EX) or 'single crystal Si' is selected for candidate material of CCM taking into account small  $|CTE|/K$  (Thermal expansion coefficient over thermal diffusivity) and large specific Young modulus. The optical performance of CCM deformed by lunar gravity or solar illumination in the holder model is presented for some cases.

Keywords: LLR, corner cube mirror, hollow, single crystal Si, deformation, optical performance

## Lunar Laser Ranging Trial at Koganei SLR station

NODA, Hiroto<sup>1\*</sup> ; KUNIMORI, Hiroo<sup>2</sup> ; ARAKI, Hiroshi<sup>1</sup>

<sup>1</sup>National Astronomical Observatory of Japan, <sup>2</sup>National Institute of Information and Communications Technology

**Introduction:** The Lunar Laser Ranging (LLR) is a technique to measure the distance between laser stations on the Earth and retroreflectors on the Moon, by detecting the time of flight of high-powered laser emitted from the ground station. Since the Earth-Moon distance contains information of lunar orbit, lunar solid tides, and lunar orientation and rotation, observation data of LLR have contributed to the lunar science, especially for the estimation of the inner structure of the Moon through orientation, rotation and tide. There are five retroreflectors on the Moon, Apollo 11, 14, 15 (U. S. A.), Lunokhod 1 and 2 (french-made, carried by former U. S. S. R.). The Apollo 15 has largest aperture among them, and almost 75 % of the total LLR data are from Apollo 15 site.

**System Description:** Since there is no Japanese station which can range the Moon so far, a precursor ranging experiment by using the Satellite Laser Ranging (SLR) facility in the NICT Koganei campus in Tokyo is ongoing. The SLR station has a 1.5 m Cassegrain telescope with Coude focus. Normally it is equipped with a laser with 20mJ, 20Hz repetition rate, and 35 picoseconds pulse width for satellite ranging. In addition to it, a wide-pulse width laser (3 nanoseconds, which corresponds to 45 cm in 2-way range) with energy of about 350 mJ per shot, repetition rate of 10Hz, wavelength of 532 nm is introduced to detect photons from the lunar retroreflectors for demonstration. As the pulse width is broad, the high accuracy ranging is not expected, therefore it is solely used for the confirmation of the optical link budget between the ground station and retroreflectors on the Moon. As the photon detector, we use a SPAD (Single Photon Avalanche Diode) and also an MCP (Micro Channel Plate) photo multiplier whose quantum efficiency is twice as much as that of the SPAD in use. For the pointing, a CCD imager is also available in the same detector box. They can be switched by reflecting mirrors. To suppress the background noise, a bandpass filter (0.3 nm FWHM, 50 % transparency) and spatial filter (pinhole) with diameter of 400 microns are installed and checked. For better link budget, the contamination of optical elements of the telescope and on the optical bench was checked. The alignment of the laser emission path with respect to the laser receiving path and laser beam divergence has been adjusted to maximize the efficiency of the laser emission.

**Pointing:** Because the retroreflectors are small and they are not visible from ground telescopes, we point the telescope to known small-sized craters (~10 km in diameter) whose positions are known in selenographic coordinate and thus in topocentric coordinate at the observation site. Then the offset angles in azimuth and elevation direction from the predicted pointing direction are determined so that the center of the crater comes to the center of the CCD images which are colligned with the SPAD and the MCP. This procedure confirms the pointing of the telescope.

**Observations:** Trials for the lunar return have been conducted since autumn 2013. As of the date of submission, the ranging to the Moon is not successful. Therefore we need to detect the return from the Apollo 15 site by using the nanosecond laser pulse for the first step. As the next step, we need to know the condition on which lunar ranging is successful in Koganei, for example, lunar phase, distance to the retroreflectors, libration angles, and atmospheric conditions.

**Keywords:** Lunar Laser Ranging, Satellite Laser Ranging, Moon, internal structure

## SELENE-2/Lunar ElectroMagnetic Sounder (LEMS): a test of inversion

MATSUSHIMA, Masaki<sup>1\*</sup> ; SHIMIZU, Hisayoshi<sup>2</sup> ; TOH, Hiroaki<sup>3</sup> ; YOSHIMURA, Ryohei<sup>4</sup> ; TAKAHASHI, Futoshi<sup>1</sup> ; TSUNAKAWA, Hideo<sup>1</sup> ; SHIBUYA, Hidetoshi<sup>5</sup> ; MATSUOKA, Ayako<sup>6</sup> ; ODA, Hirokuni<sup>7</sup> ; OGAWA, Kazunori<sup>6</sup> ; TANAKA, Satoshi<sup>6</sup>

<sup>1</sup>Tokyo Institute of Technology, <sup>2</sup>ERI, University of Tokyo, <sup>3</sup>Kyoto University, <sup>4</sup>DPRI, Kyoto University, <sup>5</sup>Kumamoto University, <sup>6</sup>ISAS/JAXA, <sup>7</sup>AIST

Understanding of lunar origin and evolution can be advanced through investigation of the lunar interior structure. The present thermal state of the Moon can be clues to the Moon's thermal history. In the SELENE-2 mission, we propose a lunar electromagnetic sounder (LEMS) to estimate the electrical conductivity structure of the Moon, which can be used to deduce the thermal structure of the Moon.

Temporal variations in the magnetic field of lunar external origin induce eddy currents in the lunar interior depending on the electrical conductivity structure and frequencies of the temporal variations. The eddy currents, in turn, generate temporal variations in the magnetic field of lunar internal origin. Therefore electromagnetic response of the Moon is obtained from magnetic field measurements by magnetometers onboard a lunar orbiter and a lunar lander. The response function is then used to estimate the electrical conductivity structure by solving an inverse problem. Here we assume a one-dimensional structure for electrical conductivity distribution. We show some results for a test of inversion.

## Moonquake observation and lunar interior exploration by one penetrator station

YAMADA, Ryuhei<sup>1\*</sup> ; ISHIHARA, Yoshiaki<sup>2</sup> ; KOBAYASHI, Naoki<sup>2</sup> ; MURAKAMI, Hideki<sup>3</sup> ; SHIRAISHI, Hiroaki<sup>2</sup> ; HAYAKAWA, Masahiko<sup>2</sup> ; TANAKA, Satoshi<sup>2</sup>

<sup>1</sup>National Astronomical Observatory of Japan / RISE Project, <sup>2</sup>Japan Aerospace Exploration Agency, <sup>3</sup>Kochi University

The penetrator developed through Japanese lunar explorer 'LUNAR-A' mission is system to deploy on-board sensors on the planetary surface by free-fall from an orbiter. The penetrator is smaller and lighter than typical soft-landers because it does not require complicated landing system and thermal control system, and it has an advantage to construct geophysical network on the planetary surface. However, on-board sensors require high shock durability to survive a penetrating impact. Through previous studies, we have already shown that seismometers for the penetrator can maintain the performance to detect moonquakes even after a shock over the impact to the lunar surface (Yamada et al., 2009) and the communication instrument on the penetrator properly operate for data transmission (Tanaka et al., 2010).

Although high shock durability of the penetrator was established, deployment of the penetrator has not been executed due to cancel of the LUNAR-A mission. We, therefore, have a plan to load the penetrator on a small satellite launched by the Epsilon Launch Vehicle. In the plan, we can carry only one penetrator due to strict weight limitation of the vehicle. For the reason, we currently study the expected scientific results obtained from the observation by one penetrator station.

The seismometers deployed through the NASA Apollo missions have detected some types of moonquakes; deep moonquake, shallow moonquake and meteoroid impacts. The seismometer for the penetrator has performance capable of observing these moonquakes, and verification of activities of these lunar seismic events through comparison with results from the Apollo mission will be one of important topics. Then, we can expect to obtain information about the lunar crustal thickness and structure if we can locate meteoroid impacts by their impact flashes from ground observation. In this presentation, we report that expected detection numbers of the lunar seismic events can be observed by the penetrator and the scientific results, and appropriate installation locations of the one penetrator to obtain good scientific results be described. Then, we also discuss the prospects for future network observation using the penetrator after the small satellite exploration.

Keywords: Penetrator, Moonquake Observation, Lunar Interior Exploration, Small Satellite Exploration, Meteoroid Impact Flash

## On the attenuation of reflected echoes of Lunar Radar Sounder onboard Kaguya

TOH, Hiroaki<sup>1\*</sup> ; KUMAMOTO, Atsushi<sup>2</sup>

<sup>1</sup>Graduate School of Science, Kyoto University, <sup>2</sup>Graduate School of Science, Tohoku University

The successful Japanese Moon probe, KAGUYA, was equipped with a variety of state-of-the-art scientific instruments including the Lunar Radar Sounder (LRS; Ono et al., 2010). LRS is a frequency modulated continuous wave (FMCW) radar with carrier frequencies from 4 to 6 MHz, and succeeded in observing distribution of reflectors beneath almost all the Moon's surface (Ono et al., 2009). Pommerol et al. (2010) further pointed out that the presence of the reflectors in lunar maria is negatively correlated with abundance of TiO<sub>2</sub> because of its high electrical conductivity.

Loss tangent is defined as a ratio of the conduction to displacement current within an electric medium and hence an indicator of high electrical conductivity. If loss tangent is small enough, the permittivity and the electrical conductivity of the Moon's surface can be determined at the same time by comparing the reflected echo of LRS with its source pulse. Namely, by estimating the complex ratio of the received signal to the transmitted pulse, the dielectric constant can be known from the phase difference while the electrical conductivity can be derived by the observed amplitude attenuation and the permittivity obtained from the phase difference.

However, determination of the complex ratios is not straightforward because the reflected echoes are the product of a pulse compression technique and thus needs deconvolution to restore the true amplitude and phase of the echoes. Preliminary analysis of the LRS waveform data collected at the end of the fast down-link (21.3 Gbps) mode [Jun. - Sep. 2008] showed that quality of the data is sufficient enough to perform necessary deconvolution. This implies that LRS can also be used as a ground penetrating radar.

In this presentation, the principle and the method for estimating the permittivity and electrical conductivity are first described in addition to the data used. Interpretation of the derived complex ratios and its spatial distribution on the Moon's surface is finally discussed and summarized.

### REFERENCES

Ono, T. et al., Lunar Radar Sounder Observations of Subsurface Layers Under the Nearside Maria of the Moon, *Science*, 323, 909-912 doi:10.1126/science.1165988, 2009.

Ono, T. et al., The Lunar Radar Sounder (LRS) onboard the KAGUYA (SELENE) spacecraft, *Space Sci. Rev.*, 154, 145-192, doi:10.1007/s11214-010-9673-8, 2010.

Pommerol, A. et al., Detectability of subsurface interfaces in lunar maria by the LRS/SELENE sounding radar: Influence of mineralogical composition, *Geophys. Res. Lett.*, 37, L03201, doi:10.1029/2009GL041681, 2010.

Keywords: Ground penetrating radar, Electrical conductivity, Permittivity, Source pulse, Reflected echo, Loss tangent

## The accumulation ages of subsurface layer in Mare Imbrium based on the SELENE observation data

ISHIYAMA, Ken<sup>1\*</sup> ; KUMAMOTO, Atsushi<sup>1</sup> ; NAKAMURA, Norihiro<sup>1</sup>

<sup>1</sup>Graduate School of Science, Tohoku University

Lunar Radar Sounder (LRS) onboard SELENE succeeded in detecting the electromagnetic wave reflected at subsurface layer in low-titanium regions [Ono et al., 2009; Pommerol et al., 2010]. Multiband Imager (MI) and Terrain Camera (TC) onboard SELENE respectively investigated the lunar surface composition [e.g., Otake et al., 2012] and the eruption ages of lunar lava flows [e.g., Morota et al., 2011]. Besides, the studies combined the LRS, MI, and TC data revealed the subsurface structure around the impact crater [Oshigami et al., 2012], and suggests the brittle subsurface layer with a high-porosity [Ishiyama et al., 2013]. This study investigates the accumulated age of subsurface layer in lava flow units (Unit 12 and 8 [Bugiolacchi and Guest, 2008]) in the north Mare Imbrium. This investigation is significant for discussing lunar volcanic activity because we can estimate a eruption rate of lunar lava flow.

We identified three subsurface echoes under Unit 8 from the LRS data, and revealed that the margin of the deepest subsurface echo was consistent with the surface boundary between Unit 12 and Unit 8; Unit 8 is accumulated on Unit 12. These ages of the units were estimated to be  $3.31 \pm 0.19$  Ga [Bugiolacchi and Guest, 2008]. However, the previous study estimated these ages by using a lunar map data with a low spatial resolution (60 – 150 m/pixel). This low spatial resolution data causes a large error for estimating the age. Thus, this study used the lunar high-resolution ortho map data obtained from TC, which has 10 m/pixel. The age of Unit 12 was estimated to be  $\sim 3.6$  Ga, which was older than the age of Unit 8. This result is consistent with the order of the stratification identified from the LRS data.

In addition, we identified that Unit 8 can be divided into several units by using the plagioclase, FeO, and TiO<sub>2</sub> Map data, produced from the MI data. We investigate the correspondence relationship between the subsurface echoes and the identified units, and then the history of lunar volcanic activity will be discussed in the presentation.

## Experimental evidence for the deep high-Ti basalt magma in the lunar mantle

IGARASHI, Mako<sup>1\*</sup> ; SUZUKI, Akio<sup>1</sup> ; OHTANI, Eiji<sup>1</sup> ; ASAHARA, Yuki<sup>1</sup> ; SAKAMAKI, Tatsuya<sup>1</sup>

<sup>1</sup>Division of Earth and Planetary Materials Science, School of Science, Tohoku University

The existence of high seismic attenuation zone at the depths greater than about 800 km implies that the lower mantle of the Moon could be partially molten (Nakamura et al., 1973; 1974). There is a longstanding hypothesis that the last fraction of the lunar magma ocean crystallized into a layer of dense Ti-rich cumulates at the shallow depths (~100 km) early in the lunar history. It has been suggested that the cumulates subsequently sank into the deep interior of the moon because of its gravitational instability (e.g., Ringwood and Kesson, 1976). It is necessary to investigate the melting relations of the high-Ti basalt that may be erupted from the depths at high pressure (>4 GPa). In this study, melting relations of Apollo 14 black glass (Delano, 1986), the most Ti-rich lunar ultramafic glasses, were experimentally determined at the pressure of 4 GPa and the temperature range from 1300 C to 1450 C.

The high-pressure and high-temperature experiments were performed by using 3000 ton Kawai-type multi-anvil apparatus of Tohoku University. The samples were packed into graphite capsules and the experimental temperatures were measured by using W-Re thermocouples. The compositions of run products were analyzed by using FE-SEM (Field Emission Scanning Electron Microscopy). Our experiments depicted that the liquidus and solidus temperatures were determined to be 1450 C and 1325 C respectively at 4 GPa.

The liquidus phase is garnet, and the first consuming phase is ilmenite. Estimated temperature profile of the Moon at depths of 700 km -1200 km are between 1100 C and 1400 C (e.g., Gagnepain-Beyneix et al., 2006). The densities of partial melts and total melt were calculated by using the partial molar volume of the oxide components at one atmosphere (Lange and Carmichael, 1987) and the Birch-Murnaghan equation of state (Sakamaki et al., 2010). The densities of the melts formed by partial and total melting of the Apollo 14 black glass were heavier than those of the lunar deep mantle. Crystal-liquid density crossover is inevitable at the depth around 800 km, the pressure corresponding to 4 GPa. Therefore, the high-Ti basalt magma can exist stably if the lunar temperature profile is close to the upper bound of the estimated lunar temperature profile, suggesting existence of the low-velocity and low attenuation anomalies caused by chemical heterogeneities in the lunar deep mantle.

Keywords: high pressure, lunar mantle, high-Ti basalt, mantle over turn

## History of heavenly bodies collision of the solar system inside of the past one billion years studying from a lunar crater

KATO, Mami<sup>1\*</sup> ; MOROTA, Tomokatsu<sup>1</sup>

<sup>1</sup>Nagoya University Graduate School of Environmental Studies

The moon preserve the record of the bodies impact history of the past 4.0 Ga as a crater, it is important the information to solution impact and orbit evolution of the bodies of the solar system.

Standard lunar cratering chronologies have been based on combining Luna and Apollo sample radiometric ages and impact crater densities. However, the bombardment history cannot be resolved in the past 3.0Ga because of the absence of samples with radiometric age ranging from 3.0 to 1.0 Ga. On the other hand, from crater density of lunar rayed craters, radiometric ages of lunar glass spherules, and statistics of terrestrial craters it has been suggested the hypothesis that the production function has increased in recent.

In this study, we determine formation ages of rayed craters using SELENE image data. Based on the finding, we will discuss a temporal variation of the cratering rate in the past 1.0 Ga.

Keywords: Moon, crater, cratering chronology

## Formation process of linear gravity anomalies and thermal evolution of the Moon

SAWADA, Natsuki<sup>1\*</sup>; MOROTA, Tomokatsu<sup>1</sup>; ISHIHARA, Yoshiaki<sup>2</sup>; HIRAMATSU, Yoshihiro<sup>3</sup>

<sup>1</sup>Graduate School of the Environmental studies, Nagoya University, <sup>2</sup>JAXA, <sup>3</sup>Graduate School of Natural Science and Technology, Kanazawa University

The investigation of the subsurface structure in the Moon through a gravity distribution is one of means to understand the early evolution history of the Moon. Andrew-Hanna et al. (2013) analyzed gravity data, obtained by GRAIL (The Gravity Recovery and Interior Laboratory) and identified linear gravity anomalies (LGAs). They suggested that the LGAs resulted from ancient intrusions formed by magmatism with globally expansion. We can expect that such intrusions leave other evidences on the surface. In this study, we analyze topography data and FeO concentration distribution to find some characters corresponding to the LGAs and magma intrusion, and, together with the thermal history of the Moon, discuss the formation process of the LGAs on the Moon.

In this study, we focus 20 of LGAs reported by Andrew-Hanna et al. (2013) that show clear gravity anomaly. We use the 1/1024-degree gridded lunar topographic data from LOLA and the 10pixel/degree lunar FeO concentration distribution map from Clementina.

For topography data analysis, we set a study area that ranges 300km in orthogonal direction from a LGA. We apply a filter to remove topographical perturbation due to small craters. On a vertical profile to a LGA, the average, the standard deviation, and the average gradient of relative altitude are calculated with a reference altitude on a LGA. We define a vicinity area as an area within 50km from a LGA and a surrounding area as an area farther than 100km from a LGA on a vertical profile. Based on topographical features of both a vicinity area and a surrounding area, we categorize the topographic feature of LGAs into three types: mountain type, valley type, and unclassified type.

For FeO concentration data analysis, we calculate the average and the standard deviation of FeO concentration in vicinity areas of a LGA from the FeO concentration map.

The topographical data analysis reveals that most of the LGAs regions are categorized as the valley type. This result suggests that the LGAs regions are distributed over trough regions formed by tensile stress in the early history of the Moon. The FeO concentration distribution analysis reveals that the average FeO concentration of the vicinity areas in highland is  $6.72 \pm 1.62$  wt%. This value is higher than that in the highland ( $<6$  wt%) of the Moon, suggesting that an ancient intrusion is possibly exposed by later crater gardening.

We propose a following hypothesis on the formation process of the linear structures as a cause of LGAs from these results and the thermal history of Head and Wilson (1992). The stress state in the early period of the Moon is tensile stress for thermal expansion process. After crack formation due to the tensile stress before 4.0 Ga, the linear structures are formed by magma intrusion. The linear structures are covered by magmatism that forms mare during 4.0-3.0Ga. Ridges are formed in mare during 3.8-3.0Ga because of the compressive stress with the cooling of the Moon or in the impact basin. The formation of the ridges occurs in association with cracks near the linear structures.

Keywords: magmatism intrusions event, expansion, ridge, FeO concentration, Lunar topography data

## Source of the lunar magnetic anomalies estimated with the prism model

YOKOYAMA, Takashi<sup>1\*</sup> ; TAKAHASHI, Futoshi<sup>1</sup> ; TSUNAKAWA, Hideo<sup>1</sup>

<sup>1</sup>Department of Earth and Planetary Sciences, Tokyo Institute of Technology

Many magnetic anomalies have been observed on the Moon since the Apollo project, although the Moon has no global intrinsic magnetic field at present. The lunar magnetic anomalies are considered to be caused by remanent magnetization of the lunar crust. Several models of the lunar magnetic anomalies have been proposed (e.g. Hood et al., 2001, 2013; Richmond et al., 2008; Purucker et al., 2012; Nicholas et al., 2007; Hemingway and Garrick-Bethell, 2012; Wieczorek et al., 2012). However, the magnetized material and its magnetizing process have been still controversial. In the present study, we have analyzed several magnetic anomalies with the prism model, in which three dimensional position, size, horizontal direction and magnetization are parameterized. The observation data by Lunar Prospector and Kaguya at the low altitude were used in the analysis. We adapt a forward modeling approach, in which the source parameters are changed iteratively till the minimum RMS (Root-Mean-Squares) misfit between the model and data is achieved. The optimal number of the prisms for modeling is objectively determined using Akaike's Information Criterion. We will discuss possible source materials on the basis of the modeling results.

Keywords: moon, magnetic anomaly, prism source model, swirl

## Lunar Electromagnetic responses to the stepwise changes in the IMF

HIGA, Tetsuya<sup>1\*</sup>; YOSHIMURA, Ryokei<sup>2</sup>; OSHIMAN, Naoto<sup>2</sup>; SHIMIZU, Hisayoshi<sup>3</sup>; MATSUSHIMA, Masaki<sup>4</sup>; TAKAHASHI, Futoshi<sup>4</sup>; SHIBUYA, Hidetoshi<sup>5</sup>; TSUNAKAWA, Hideo<sup>4</sup>

<sup>1</sup>Graduate School of Science, Kyoto University, <sup>2</sup>Disaster Prevention Research Institute, <sup>3</sup>Earthquake Research Institute, University of Tokyo, <sup>4</sup>Department of Earth and Planetary Sciences, Tokyo Institute of Technology, <sup>5</sup>Department of Earth and Environmental Sciences, Kumamoto University

The electrical conductivity structure of the lunar interior provides us very important information for investigation of the lunar origin and evolution. We attempted to estimate on the lunar electrical conductivity from magnetic field measurements by LMAG on board KAGUYA (SELENE) during the period from 21 December 2007 to 31 October 2008, when KAGUYA was in the orbit of 100-km altitude.

Magnetic fields are induced in the moon by changes in the interplanetary magnetic field (IMF). In order to confirm whether the lunar electromagnetic induction signals are observed in KAGUYA data, we compared KAGUYA data and data of ACE and WIND satellites, which locate around the Lagrange point (Sun-Earth L1), when the stepwise changes are shown in each data. LMAG measured the sum of the inducing and the induced fields, while ACE and WIND measured only the inducing field. It was found that LMAG recorded the lunar electromagnetic responses to the stepwise changes in the IMF.

Dyal and Parkin (1971) gave the homogeneous moon model and estimated lunar conductivity. Their estimation was carried out using the data measured by Apollo 12 magnetometer fixed on the lunar surface. In this study, we applied their method to the data of the orbiting satellite, KAGUYA. The homogeneous moon model was able to explain the electromagnetic response against the stepwise changes in the IMF well, and the estimated homogeneous lunar conductivity was  $1 \times 10^{-4} - 4 \times 10^{-4}$  S/m. On the other hand, we found that LMAG data also recorded the anomalous signals in the minor components, not predicted from the above model. In order to confirm whether such signals are unique to KAGUYA data, we scrutinized the data obtained by Apollo and Lunar Prospector. As a result, we concluded that such signals are common when the stepwise changes penetrate the moon.

In this presentation, we will report the new analysis results of KAGUYA, Apollo, and Lunar Prospector data, and discuss the anomalous signals in the minor component of the responses to the stepwise changes in the IMF.

Keywords: Moon, KAGUYA, SELENE, LMAG, induction, conductivity

## Plasma observations above strong lunar crustal fields in the solar-wind wake

NISHINO, Masaki<sup>1\*</sup> ; SAITO, Yoshifumi<sup>2</sup> ; TSUNAKAWA, Hideo<sup>3</sup> ; TAKAHASHI, Futoshi<sup>3</sup> ; YOKOTA, Shoichiro<sup>2</sup> ; MATSUSHIMA, Masaki<sup>3</sup> ; SHIBUYA, Hidetoshi<sup>4</sup> ; SHIMIZU, Hisayoshi<sup>5</sup> ; FUJIMOTO, Masaki<sup>2</sup>

<sup>1</sup>Nagoya University, <sup>2</sup>ISAS/JAXA, <sup>3</sup>Tokyo TECH, <sup>4</sup>Kumamoto University, <sup>5</sup>Earthquake Research Institute, The University of Tokyo

Plasma signature around crustal magnetic fields is one of the most important topics of the lunar plasma sciences. Although recent spacecraft measurements are revealing solar-wind interaction with the lunar crustal fields on the dayside, plasma signatures around crustal fields on the night side have not been fully studied yet. Here we show evidence of plasma trapping on the closed field lines of the lunar crustal fields in the solar-wind wake, using SELENE (KAGUYA) plasma and magnetic field data at 15 km altitude. In contrast to expectation on plasma cavity formation at the strong crustal fields, electron flux is enhanced above one of the strongest crustal fields, Crisium Antipode (CA), where the magnetic field along the spacecraft orbit is as strong as 80 nT. The enhanced electron fluxes above CA are characterized by bidirectional beams in the lower energy range (typically lower than 100 eV), which shows that these electrons are trapped on the closed field lines of the crustal magnetic fields, although a possibility of opened field configuration with cusps is not totally excluded. The observed electrons on the closed field lines may come from the lunar night side surface, while the mechanism of electron supply onto the closed field line remains to be solved.

Keywords: Lunar crustal field, Lunar plasma environment, Lunar wake, SELENE (KAGUYA)

## A long-term all-sky imager observation of lunar sodium tail

NISHINO, Masaki n<sup>1\*</sup>; SHIOKAWA, Kazuo<sup>1</sup>; OTSUKA, Yuichi<sup>1</sup>

<sup>1</sup>Solar-Terrestrial Environment Laboratory, Nagoya University

The Moon possesses long tail of neutral sodium atoms that are emitted from the lunar surface and transported anti-sunward by the solar radiation pressure. Since the earth crosses the lunar sodium tail for a few days around the new moon, the resonant light emission from sodium atoms can be detected from the ground. Although it has been reported that bright emissions from sodium atoms of the tail is observed during the Leonids meteor shower, only few events without meteor shower have been investigated so far. Here we show a long-term (over 15 years) observation of the lunar sodium tail using all-sky imager at Shigaraki Observatory (35N, 136E), Japan. We have surveyed our database of all-sky sodium images at a wavelength of 589.3 nm to find that a bright spot emerges around the anti-lunar point for a few days around the new moon. Although the sodium spot is the brightest during the Leonids meteor shower, a weaker sodium spot is detected in the period without meteor shower as well. The sodium spot gradually moves eastward (roughly, 0.2 hours a day), which shows that the sodium tail is strongly affected by the earth's gravity. We will present the latest results of our data analysis to discuss signatures of the lunar sodium tail as well as the origin of the lunar sodium exosphere.

Keywords: Lunar sodium tail, Lunar exosphere, All-sky imager observation